Retrieval of the aerosol optical depth in the UV-B at Uccle from Brewer ozone measurements over a long time period 1984–2002

Anne Cheymol and Hugo De Backer

Royal Meteorological Institute of Belgium, Uccle, Belgium

[1]   Since 1984, Brewer spectrophotometer #16 has measured the ozone column at Uccle near Brussels in Belgium (50°48′N, 4°21′E, 100 m) from the direct sun observations at five isolated wavelengths in the UV-B: 306.3 nm, 310.1 nm, 313.5 nm, 316.7 nm and 320.1 nm. We have used the Langley Plot Method (LPM) to retrieve the aerosol optical depth (AOD) from these observations over a long time period: from 1984 to November 2002. A seasonal variation of the AOD is clearly observed with mean AOD values of about 0.4 and 0.9 at 306.3 nm in winter and in summer respectively. The magnitude of these AODs is comparable to the AODs measured by AERONET sunphotometers at other places. We succeeded to demonstrate the impact of the eruption of Mount Pinatubo on the retrieved AOD in the UV-B at Uccle in winter. Trend analysis on the mean annual AOD gives significant negative trends at the 2σ level only from 1989 to 2002 at all wavelengths and not over the whole period 1984–2002. The annual trend amounts to $-2.46 \pm 0.37\%$/year at 306.3 nm over 1989–2002. Significant negative seasonal trends at the 2σ level are only found in winter at all wavelengths ($-2.66 \pm 0.65\%$/year at 306.3 nm for example) and in summer at 306.3 *nm* ($-1.24 \pm 0.55\%$/year). In summer, in autumn and in spring at the other 4 wavelengths the trends are not significant at the 2σ level.   *INDEX TERMS:* 0305 Atmospheric Composition and Structure: Aerosols and particles (0345, 4801); 0370 Atmospheric Composition and Structure: Volcanic effects (8409); 0394 Atmospheric Composition and Structure: Instruments and techniques; *KEYWORDS:* aerosols, Langley plot method, UV-B

1.   Introduction

[2]   Aerosols are airborne particles or a collection of such particles. Some of them are of natural origin, like sea salt particles while others are of anthropogenic origin like dust or smoke. It was pointed out in recent years that aerosols play an important role in climate forcing in two ways. First, the scattering and the absorption of the incoming solar radiation by aerosols has a direct influence on the radiative budget of the Earth's atmosphere. Second, an indirect effect is the enhancement of cloud formation [*Houghton et al.*, 2001]. The presence of aerosols increases the cloud condensation nuclei concentration and consequently increases the absorption of UV-B radiation. In some very polluted regions, the decrease of UV-B radiation due to aerosol loading becomes larger than the increase due to the ozone decline in the atmosphere [*Liu et al.*, 1991]. *Kylling et al.* [1998] estimate that the AOD reduce the UV-B irradiance by about 5 to 35%.

[3]   Earlier studies pointed out that the aerosols absorb UV-B radiation and affect in this way the UV quantity received by Humans and the biosphere [*Wenny and Saxena*, 2001]. It is very important to quantify the absorption in the UV-B by aerosols as UV-B intensities affect human health directly, for example, via the development of skin cancer.

[4]   In the past, many reports have been written on the retrieval of aerosol optical depth in the atmosphere and their properties [*King et al.*, 1980], [*Marenco et al.*, 1997], [*Alexandrov et al.*, 2001]. Some papers tried to evaluate the AOD of the atmosphere in the UV-B and its variation with time [*Kirchhoff et al.*, 2001], to estimate the AOD in the UV [*Cachorro et al.*, 2002], or to correlate the general circulation of the atmosphere with the aerosol transport to forecast the time variation of the aerosol in the atmosphere in order to guide environmental protection policies [*Takemura et al.*, 2001]. Another way to study the AOD is to determine the aerosol single scattering albedo which is an important aerosol radiation parameter in determining surface UV irradiance [*Petters et al.*, 2003].

[5]   Several instruments are able of measuring the solar irradiance intensity in different wavelength ranges. Sunphotometers measure generally at wavelengths greater than 340 nm (like the instruments used in the network AERONET http://aeronet.gsfc.nasa.gov:8080) to avoid the effect of ozone on the solar irradiance. Brewer spectrophotometers

were developed to measure total ozone in the atmosphere and consequently measure the solar irradiance intensity in the UV-B, between 290 and 325 nm [*Brewer*, 1973]. Satellite-borne instruments like SAGE II measure the aerosol extinction at isolated wavelengths using the solar occultation technique. Another way to infer the AOD is to use a lidar, as in *Marenco et al.* [1997]. A lidar does not measure the solar irradiance but measures the backscattered signal of the laser to infer the AOD.

[6]   The focus of this study is to retrieve the AOD from raw direct sun (DS) total ozone observations performed with Brewer spectrophotometer #16. The primary task of this instrument is to measure the total ozone column at Uccle, situated near Brussels in Belgium (50°48′N, 42°1′E, 100 m) in a residential area. From these measurements, *De Muer and De Backer* [1992] demonstrated that pollution has influenced the ozone measurements performed with Dobson instrument #40 at Uccle during the 70s and 80s.

[7]   We use a simple regression method, the LPM (Langley Plot Method) to extract AOD for a long time period from 1984 to November 2002. Similar techniques were used by *Bais* [1997], *Krishna Moorthy et al.* [1998] and *Marenco et al.* [2002], but for shorter periods of time. Consequently, they could not study the time variation and the trends of the AOD as we do in this work.

[8]   Owing to the relatively long time period covered by the data used in this study, it is possible to analyze the seasonal variation of the AOD, to see if there is an impact from the Pinatubo eruption on the AOD at Uccle, to compare our results with other measurements such as in the AERONET database and to see if there are significant trends in the time series of the AOD.

2.   Instrument and Data

2.1.   Instrument Description

[9]   Brewer instrument #16 [*SCI-TEC*, 1988] is used routinely at Uccle to measure the total ozone column in the atmosphere from the direct sun (DS) ultraviolet radiation. In the UV, the extinction of the solar light depends not only on aerosols and Rayleigh scattering, but also on ozone. Consequently, the AOD cannot be inferred from a single measurement, if the ozone column is not known. Since the instrument is primarily used for ozone observations, there is no absolute calibration for the direct sun observations for each wavelength. Only the extraterrestrial constants for the ozone and SO_2 wavelength ratios are determined by the standard calibration procedure. Therefore we must use another technique to retrieve AODs. Our study is based on the direct solar irradiance intensity measured at five wavelengths in the UV-B centered at 306.3 nm, 310.1 nm, 313.5 nm, 316.7 nm and 320.1 nm.

[10]   Brewer #16 is a single monochromator version MARK II. It was installed in 1983 at Uccle. Since 1985, the calibration of this instrument has been maintained internally. For more details on the calibration method and history, see *De Backer and De Muer* [1991]. On regular basis, the Brewer makes 5 individual direct sun (DS) ozone observations within 3 minutes and 7 individual zenith sky (ZS) ozone observations within 5 minutes. In 1989, the instrument was equipped with an automated azimuth and zenith pointing system, resulting in a higher observation frequency. Before 1989, the measurements were made manually and thus their frequency was less than half of that after 1989: before 1989 we had about 6700 data per year and about 13000 data per year after 1989. The difference in density of DS observations necessitates a difference in the AOD processing of both periods: before and after 1989.

2.2.   Data Preprocessing

[11]   Before applying Beer's law (see section 3.1), the raw data consisting of photon-counts for five wavelengths have to be adjusted for the dark count, the dead time and the temperature dependence of the sensitivity of the instrument. In this paper, we consider the direct sun observations at the five wavelengths used for total ozone retrieval.

[12]   To account for low and high radiation intensities, five neutral-density filters are automatically activated to keep the signal within the sensitivity range of the photomultiplier of the Brewer. They change with the solar irradiance intensity during the day. In order to use the data corresponding to different filters on the same plot, they are adjusted by five attenuation factors corresponding to the five filters. The attenuation factors of the neutral-density filters are measured at Uccle with the internal standard lamp of the instrument. For Brewer #16, the light intensity is lowered by a factor of 2.94, 7.77 and 32.79 for filters 1, 2 and 3 respectively. These are the ones used at Uccle from 1984 to 2002. The study of *Marenco et al.* [2002] determines AOD for each filter separately and thus they have smaller zenith angle ranges for one day.

3.   Method

3.1.   Basic Equation

[13]   The signal, after adjustments for dark count, dead time and temperature, received by the Brewer spectrophotometer is governed by Beer's law:

$$S(\lambda) = K(\lambda)I_o(\lambda)exp\left[\underbrace{-\mu\alpha(\lambda, T)\Omega}_{a}\underbrace{-m\beta(\lambda)P/P_{std}}_{b}\underbrace{-\delta(\lambda)\sec(z_a)}_{c}\right]$$

(1)

where $S(\lambda)$ is the signal received by the instrument (in photon-counts per second), $K(\lambda)$ represents the proportionality factor of the instrument's response to the incoming solar radiation at wavelength λ, $I_o(\lambda)$ is the irradiance outside the Earth's atmosphere at wavelength λ, μ is the relative optical airmass of the ozone layer at height of 22 km (the mean height where the maximum of ozone in the atmosphere resides), $\alpha(\lambda, T)$ is the ozone absorption coefficient at wavelength λ and temperature T, Ω is the equivalent thickness of the ozone layer, m is the relative optical airmass of the atmosphere of a thin layer assumed to be at an altitude of 5 km for the Rayleigh scattering, $\beta(\lambda)$ is the Rayleigh scattering optical thickness of a vertical path through the atmosphere normalized to standard pressure P_{std}, P is the air pressure at the station, P_{std} is the standard air pressure (1013.25 hPa), $\delta(\lambda)$ is the aerosol scattering optical thickness of a vertical path through the atmosphere, z_a is the zenith angle of the sun.

[14]   Going through the atmosphere, the direct irradiance intensity at the top of the atmosphere is absorbed and

scattered by three different physical phenomena represented in equation (1): (1) the absorption by ozone, (2) the scattering by air molecules (Rayleigh scattering), and (3) the scattering by aerosol particles.

[15] The relative optical airmass "m" and "μ" in equation (1) for a layer at a height h above the Earth's surface can be represented in a generic form for both molecules and ozone as:

$$am(h) = \sec\left[\arcsin\left(\frac{R}{R+h}\right)\sin(z_a)\right] \quad (2)$$

where R is the mean radius of the Earth (6370 km).

[16] It is important to note that the SO_2 absorption is not considered in equation (1) because the SO_2 term is lower by a factor of more than 100 than the ozone term: the order of magnitude of the SO_2 column is lower than 3 DU (compared to about 300 DU for the total ozone column) while the ozone and SO_2 absorption coefficients are comparable [*De Muer and De Backer*, 1992]. Also, *Kirchhoff et al.* [2002] show that at La Paz, the optical depth for SO_2 is negligible.

[17] As the ozone quantity is independent of the aerosol in the atmosphere, we can infer the AOD from DS observations using equation (1). The method is described in the next section.

3.2. Langley Plot Method

[18] The aim of our study is to infer the AOD for all the direct sun ozone observations in our database in order to analyze how the AOD varies with time and to see if our results are influenced by the major volcanic eruption of Mount Pinatubo in 1991. We use the Brewer measurements of the direct solar irradiance in the UV-B, as mentioned in 2.2.

[19] The LPM is a linear regression technique applied on the equation (1) that allows us to retrieve the AOD from DS measurements. We apply the LPM as explained by *Bais* [1997], *Kirchhoff et al.* [2001], *Marenco et al.* [2002]. Taking the logarithm of equation (1), we obtain the following equation:

$$\underbrace{lnS(\lambda) + \mu\alpha(\lambda)\Omega + m\beta(\lambda)P/P_{std}}_{Y} = \underbrace{ln[K(\lambda)I_o(\lambda)]}_{CF} - \underbrace{\delta(\lambda)}_{A}\underbrace{\sec(z_a)}_{X}$$

$$(3)$$

In simplified form:

$$Y = CF - A * X \quad (4)$$

where $Y = lnS(\lambda) + \mu\alpha(\lambda)\Omega + m\beta(\lambda)P/P_{std}$.

[20] It gives only one estimation of the AOD and one calibration factor (CF) per day and per wavelength. Since the Brewer measures at 5 wavelengths, we will have 5 AODs and 5 CFs for one day.

[21] The calibration factor is defined as $CF = ln[K(\lambda)I_o(\lambda)]$. It is the intersect of the fitting line with the Y axis on the graph. Physically, it represents the extraterrestrial constant of the instrument for observation of AOD.

[22] $A = \delta(\lambda)$ is the AOD which is the slope of the fitting line; $X = \sec(z_a)$ is the X axis. The quality of the linear regression obviously depends on the range of the $\sec(z_a)$ that is covered. In other words, a good linear regression can
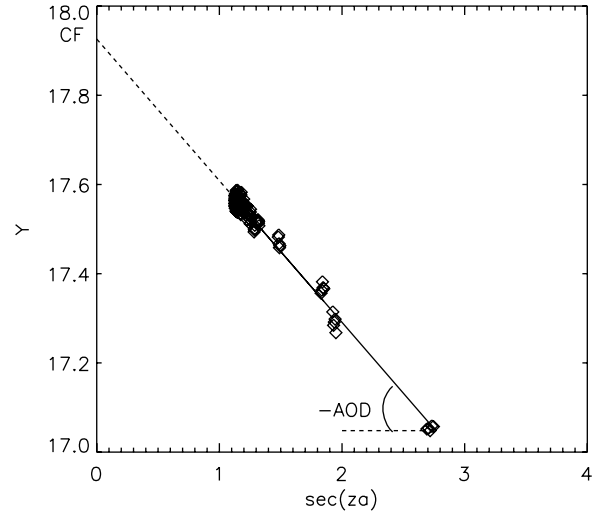
Figure 1. Langley Plot Method applied on the CD 18 June 2000 for 306.3 nm. The solid line is the linear regression and each diamond is a couple of (X, Y) for one time. The calibration factor, CF (17.98), is the intersect of the line with Y axis and the slope is equal to -AOD (0.32).

only be obtained if we have good DS observations both at low and high solar zenith angle: the number of daily data have to be distributed over the whole day in a wide range of zenith angles. Also the atmospheric conditions have to be stable over the day. Therefore we have to select days on which the LPM can be applied.

[23] We select these days with the following criteria:

[24] 1. The individual direct sun ozone observations are performed 5 times in 3 minutes. The ozone column and standard deviation is computed on such a group of five individual DS measurements for each wavelength. Data are accepted if the standard deviation is lower than 2.5 DU.

[25] 2. the range of zenith angles covered by valid DS observations (following criterion 1) on one day must be at least 20°.

[26] 3. the number of the individual DS data (fulfilling the two previous criteria) must be at least 50 (i.e 10 sequences of 5 observations).

[27] The first criterion is to test the individual DS data: if it is not verified, it means that during the measurement the cloud conditions changed and that we cannot be sure that the solar irradiance is not absorbed by the water vapor in the clouds. The second and the third criteria guarantee that there are enough data all over the day on which the LPM is applied. The days which fulfill these three criteria are called in this paper "Cloudless Days" (CD).

[28] Figure 1 shows for 18 June 2000 the CF and the AOD value (the opposite of the slope) for 306.3 nm. For this day, CF is 17.98 and the AOD is 0.32 (unitless). There are 115 individual DS data (or 23 groups of 5 individual scans) on this day to determine the CF and AOD. The solid black line is a least absolute deviation regression which is the result of equation (4). A least absolute deviation regression is used because it is less sensitive to the outliers. The AOD and CF are inferred in the same way for the other 4 wavelengths. With this method we can obtain the AOD on CD.

Table 1. Mean Value of the Five CFs From the LPM on 35 LPD for Brewer #16 From 1989 to 2002 and 47 CD1515 From 1984 to 1988

Wavelength, nm	CF 37 CD1515 1984–1988	CF 35 LPD 1989–2002
306.3	17.75 ± 0.30	18.01 ± 0.19
310.1	17.55 ± 0.31	17.76 ± 0.19
313.5	18.01 ± 0.32	18.18 ± 0.20
316.7	17.84 ± 0.32	18.02 ± 0.19
320.1	17.63 ± 0.32	17.84 ± 0.19

[29] The second stage is to retrieve AOD for all the days for which we have DS observations, including days that do not fulfill the criteria for CD. As the linear regression cannot be used here, the only way to obtain the AOD is to make use of a fixed CF in equation (4) as it will be explained in the next section.

[30] In the following sections, most of the plots only represent 2 of the 5 wavelengths: 306.3 nm and 320.1 nm. The results for the other wavelengths are quite similar.

3.3. Stability of the Calibration Factor

[31] To be sure about the stability of the atmospheric conditions during the considered days, all Langley plots from CD data set are individually visualized to verify that the data are quasi on a straight line. There was only one CD before 1989. Indeed, until 1989, the Brewer measurements were made manually and consequently there are too few data for each day to verify the third condition (see 3.2) of the CD. Thus the group of CD only represents the period 1989–2002. In 35 days, the conditions where favorable with data which are grouped well on lines: these days are called "Langley Plot Days" (LPD). The average CF obtained from this subset of 35 LPD are given in Table 1, last column.

[32] The standard deviations on the five CF are small compared to the CFs values. This means that the estimation of the mean CF did not vary much over the period considered here. To estimate the error on the mean CFs values, we calculate the standard deviation of the mean CFs estimation, and we divide it by the square root of the number of data. At all wavelengths, this is equal to 0.03 over the period 1989–2002. This number represents an upper limit (at $secz_a = 1$) of the contribution of the error on the mean CF to the AOD error.

[33] As there are only CD from 1989 to 2002, it is very important to verify whether from 1984 to the end of 1988, the CF are not significantly different from the values in Table 1, 3nd column. The mean value of the CF over the period 1984–1988 for the 5 wavelengths are given in Table 1, 2nd column. To have some days in this period, we weaken the 2nd and 3rd criteria (see 3.2): the range of zenith angles must be at least 15 and the number of the individual DS data must be at least 15 (i.e., 3 sequences of 5 observations). We call these days CD1515. The CF obtained are shown in Figure 2, asterisks represents the CD1515 and diamonds represent the CD. From Table 1 and Figure 2, we conclude that the mean value of the CF from 1984 to 1988 does not differ significantly from the values over the 1989–2002 period, that there is no trend in the CF (see Figure 2). Linear regression on the CF for the period 1989–2002 gives trends (see Figure 2) that are not

significant at the 2σ level: for example, the trend is about 0.05 ± 0.03%/year at 306.3 nm. The same conclusion can be made over the period 1984–2002. Therefore the CFs can be considered constants for each wavelength.

3.4. Resulting Data Set

[34] The LPM is used to determine the 5 CFs of the Brewer instrument. After fixing the CFs, it is possible to calculate the AOD for DS measurement. On the basis of the criteria in section 3.2, 418 daily values of the AOD were calculated with the LPM method. The days selected are mainly in spring (in March 5.3%, in April 12.2% and in May 20.6% of the total), in summer (in June 17.0%, in July 15.8% and in August 20.6% of the total) and in autumn (in September 8.6%). This distribution is related to the larger range of zenith angles during spring, summer and the beginning of autumn and thus, there are more data for these periods. These days are only from 1989 to 2002 except for one day in 1984. Within these 418 data, we select 35 CD and we average the 35 values of the 5 CFs to have 5 mean values of CFs.

[35] The second step of the study is to compute the AOD for every DS data in fixing the CFs. With this method we have several values of AOD per day. The purpose of our study is to evaluate the time variation of the AOD over a long time period. To that end, we calculate the daily mean AODs. Finally, 3741 values of daily mean AOD are available from 1984 to 2002.

4. Sensitivity of the AODs Retrieval Method to the Ozone and the Effective Ozone Temperature in the Atmosphere

4.1. AOD Sensitivity to the Ozone

[36] The absorption of solar radiation in the UV depends strongly on ozone and so does our retrieval AOD method. To determine the error on the AOD due to the error on the ozone measurement, we compare the relative differences between AODs calculated with a constant ozone column of 330 DU and those obtained with the ozone column as
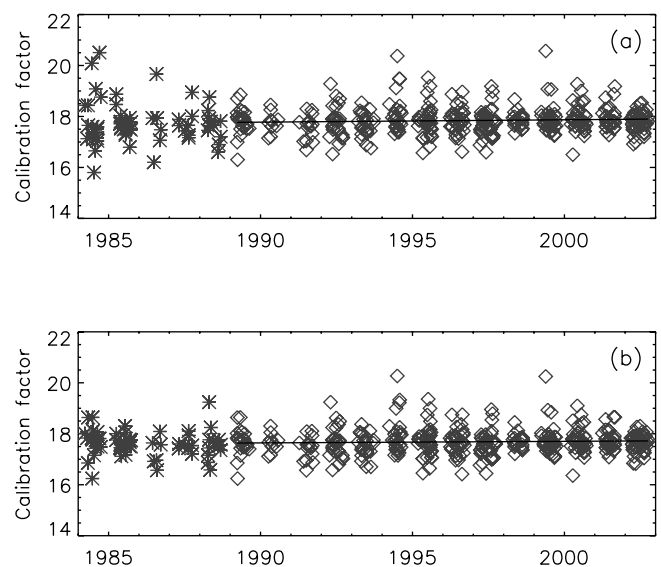
Figure 2. Time series of the 2 CFs for (a) 306.3 nm and (b) 320.1 for Brewer #16 over 1984–2002.
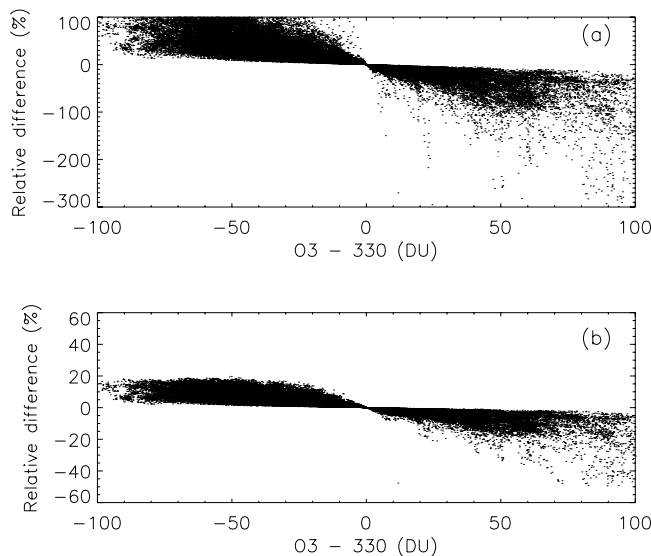
Table 2. Sensitivity of the AODs to the Ozone[a]

Wavelength, nm	Slope, %/DU	Stdev, %/DU
306.3	−0.9528	±0.0023
310.1	−0.4901	±0.0009
313.5	−0.3830	±0.0008
316.7	−0.1757	±0.0003
320.1	−0.1594	±0.0003

[a]The values are the slopes of the linear regression of the relative difference between the AODs determined with and without the use of the variation of the ozone in the atmosphere.

Table 3. Contribution of the Error on the CF's and on Ozone's Variation of 3 DU to the Error on the AOD's Error and the Total of These Two Contributions

Wavelength, nm	Error on Ozone, Unitless	Error on CFs, Unitless	Total Error, Unitless
306.3	0.027	0.03	0.057
310.1	0.013	0.03	0.043
313.5	0.010	0.03	0.040
316.7	0.005	0.03	0.035
320.1	0.004	0.03	0.034

measured with Brewer #16. For this purpose, we do not compare daily means but the individual observations: Thus we have 88917 data. Table 2 summarizes the slopes of the lines in Figure 3 (where we only show results for 2 wavelengths). The sensitivity of the AOD retrieval is, as expected, higher at 306.3 nm than at the other wavelengths. This clearly shows the need of total ozone data to retrieve AODs at these short wavelengths. We can also estimate the contribution of the error on the ozone measurement (typically 1% or about 3 DU for a well calibrated Brewer instrument). The contribution of the ozone's error to the mean value of AOD for 306.3 nm is about 0.004 in Winter (the mean AOD value in this season is about 0.4) and for Summer it is about 0.009 (the mean AOD is about 0.9) per Dobson Unit. At 306.3 nm a difference of 3 DU causes an error of about 0.012 on the AOD in Winter and 0.027 in Summer: it means that there is an error of about 3% on the AOD. At 320.1 nm, an error of 3 DU on ozone column causes an error on the AOD of about 0.0018 and 0.004 on a mean value of 0.40 in Winter and 0.88 in Summer respectively: it represents an error of about 0.4% on the AOD.

[37] This means that the contribution of the error on ozone to the AOD retrieval is negligible at 320.1 nm but is important at 306.3 nm. Table 3 summarizes the maximum

Figure 3. Relative differences between the AODs determined with and without the use of the variation of the ozone in the atmosphere for (a) 306.3 nm and (b) 320.1 nm. Note the different scale of Figures 3a and 3b.

contribution (corresponding to summer) of the error on CFs and ozone to the AODs. Last column of this table represent the error due to the error on ozone and CF for each wavelength to the AOD: it is calculated according to the following equation:

$$b_i CF_i \pm \sigma_i - b_{i+1} CF_{i+1} \pm \sigma_{i+1} = b_i CF_i - b_{i+1} CF_{i+1} \\ \pm \sqrt{(b_i)^2 \sigma_i^2 + (b_{i+1})^2 \sigma_{i+1}^2} \quad (5)$$

where b is a multiplication factor,

[38] Most of the error is due to the error on the CFs except at 306.3 nm for which the error on the ozone is similar to the error on the CFs.

4.2. Sensitivity to the Effective Ozone Temperature

[39] Calculated AODs and CFs depend on the effective ozone temperature through the dependence of the ozone absorption coefficient (equation (1)) on temperature. Equation (6) gives the relation between the ozone absorption coefficient and the effective ozone temperature [*Bass and Paur*, 1985] using the ozone cross section:

$$\alpha(\lambda, T) = \frac{P_{std} N_a \sigma(\lambda, T_{deg})}{R T_{std}} 10^{-6} \quad (6)$$

where $\alpha(\lambda, T)$ is the ozone absorption coefficient at wavelength λ and temperature T(°K) in $[atm.cm]^{-1}$, N_a is the Avogadro's number ($6.0225.10^{23} molec.mole^{-1}$), R is the gas constant (8.314 in $J.K^{-1}.mole^{-1}$), T_{std} is the standard temperature (273.15 K), P_{std} is the standard pressure ($1013.25.10^2 Pa$).

[40] *Bass and Paur* [1985] give the ozone cross section as follows:

$$\sigma(\lambda, T_{deg}) = \left[C_0(\lambda) + C_1(\lambda) T_{deg} + C_2(\lambda) T_{deg}^2 \right] 10^{-20} \quad (7)$$

where $\sigma(\lambda, T_{deg})$ is the cross section in cm^2 at wavelength λ and effective temperature T_{deg}(°C), C_0, C_1 and C_3 are the quadratic coefficients at wavelength λ from *Bass and Paur* [1985].

[41] The sensitivity of the calculated AOD and the CF to the effective ozone temperature is tested in the next paragraphs.

[42] The stratospheric effective ozone temperature is the convolution between the air temperature profile and the ozone profile, as pointed out by *Van Roozendael et al.* [1998]. In order to study the sensitivity of the retrieved AODs to the effective ozone temperature, the effective ozone temperature is calculated from soundings performed
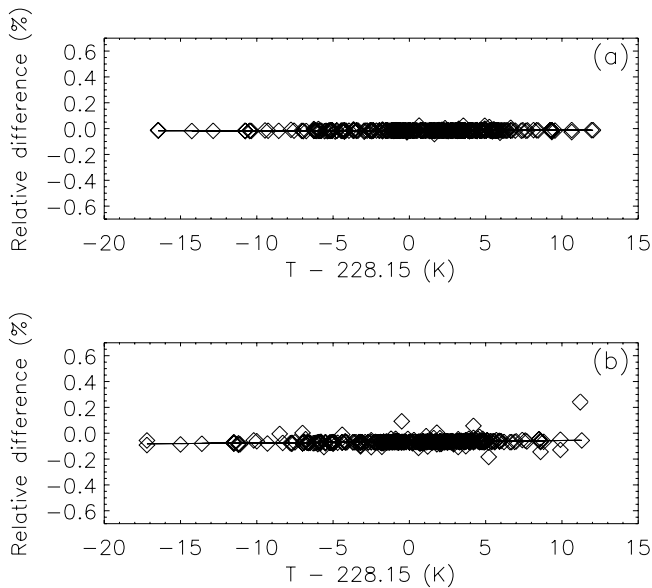
Figure 4. Relative differences between the CFs determined with and without the use of the variation of the effective ozone temperature for (a) 306.3 nm and (b) 320.1 nm.

Figure 5. Relative differences as Figure 4 but for AODs for (a) 306.3 nm and (b) 320.1 nm. Note the different scale of Figures 5a and 5b.

at Uccle. Ozone and air temperature profiles are measured at Uccle three times a week. On days without sounding the effective ozone temperature is replaced by the monthly mean effective temperature which is calculated for the whole period 1984–2002.

[43] In order to test the sensitivity of the AOD and CF to the effective ozone temperature, we compare the AOD obtained with a calculated effective ozone temperature and a standard effective ozone temperature equal to 228.15 K [*Van Roozendael et al.*, 1998].

[44] From 1984 to 2002, the effective ozone temperature on 3741 data ranges from 207.3 K to 243.1 K with a mean value of 225.7 ± 5.6 K. The effective ozone temperature deviates up to −21 K and +15 K from the mean standard effective ozone temperature.

[45] In the next section, a dependence of the CF and the AOD on this temperature interval is represented to test the sensitivity on the effective ozone temperature.
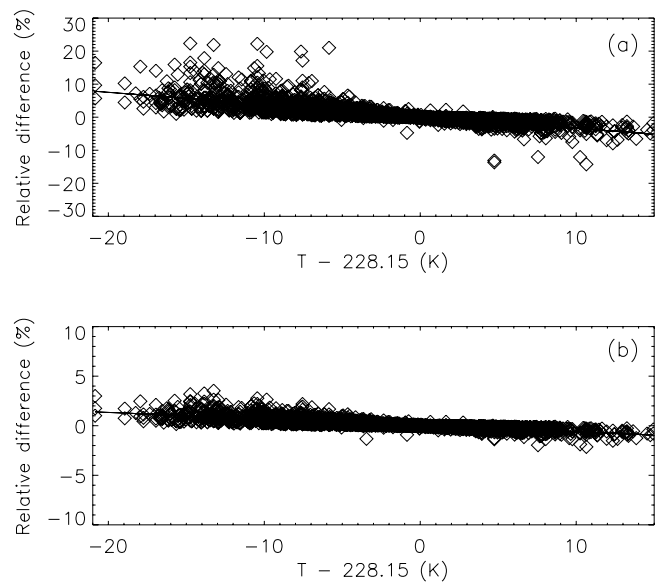
4.2.1. Calibration Factor Sensitivity

[46] Figure 4 shows, at 306.3 nm and 320.1 nm, the relative difference between the CF (corresponding to the 418 CD data) obtained using computed and estimated effective ozone temperature and the CF obtained using a standard effective ozone temperature equal to '228.15 K'. It is represented as a function of the difference between the effective ozone temperature and the standard temperature.

[47] The slopes of the best fitting lines shown in Figure 4 are listed in Table 4. The differences of the CF are

significant at the 2σ level for all wavelengths. However, they are very small compared to the order of magnitude of the CF. For the biggest difference in fact 15°C, the error on the estimation of the mean CF for 306.3 nm is about 0.002 (e.g., 0.01 divided by the square root of the number of CFs) which is smaller to the error on the mean CF which is 0.03.

[48] Therefore this increase can be neglected and thus, the effective ozone temperature has no significant impact on the CF.

4.2.2. Aerosol Optical Depth Sensitivity

[49] Figure 5 shows the relative difference between the AOD computed with the measured and standard effective ozone temperature as a function of the difference between these two temperatures. In Figure 5, 3741 are shown corresponding to CD inferred with fixed CF. Least chi-square linear regression lines are also shown and the regression coefficients are given in Table 5. These coefficients represent the sensitivity of the AOD to the effective ozone temperature in %/K. At all wavelengths, the AOD dependencies are significant at the 2σ level. The difference is larger at 306.3 nm.

[50] The most striking feature of Figure 5 is the number of points at 306.3 nm showing differences of 15% and more. These points correspond to days with low AOD (lower than 0.1). Therefore with such small values of AOD, a small difference introduced by a dependence on the effective ozone temperature induces a large relative

Table 4. Sensitivity of the Calculated CFs to the Effective Ozone Temperature From the LPM on 418 CD

Wavelength, nm	Slope, %/K	Stdev, %/K
306.3	−0.0054	±0.0014
310.1	−0.0037	±0.0012
313.5	−0.0084	±0.0006
316.7	−0.0013	±0.0005
320.1	−0.0009	±0.0003

Table 5. Sensitivity of the AODs to the Effective Ozone Temperature[a]

Wavelength, nm	Slope, %/K	Stdev, %/K
306.3	−0.363	±0.004
310.1	−0.254	±0.003
313.5	0.091	±0.001
316.7	−0.098	±0.001
320.1	−0.065	±0.001

[a]The values are the slopes of the linear regression in Figure 5.

Table 6. Mean Monthly AODs at Uccle for 320.1 nm in 1995 and 2001, From Our Calculation, and From AERONET at Lille for 340 nm in 1995 and at Ostende for 340 nm in 2001[a]

Months	Uccle 320.1 nm	Lille 340 nm, 1995	Ostende 340 nm, 2001
Jun95	0.82 ± 0.41	0.39 ± 0.13	
Jul95	0.99 ± 0.40	0.60 ± 0.24	
Aug95	1.00 ± 0.37	0.41 ± 0.23	
Sep01	0.75 ± 0.36		0.40 ± 0.31
Oct01	0.55 ± 0.30		0.25 ± 0.15
Nov01	0.32 ± 0.14		0.16 ± 0.04
Dec01	0.19 ± 0.05		0.11 ± 0.02

[a]AERONET data available at http://aeronet.gsfc.nasa.gov:8080.

difference on the AOD as can be seen in Figure 5a. The AOD sensitivity to the effective ozone temperature at the 5 wavelengths is summarized in Table 5.

[51] It appears that the effective ozone temperature has a larger impact on the AOD at 306.3 nm than at other wavelengths. This is due to the larger ozone cross section at this wavelength (see section 4.2 *Bass and Paur* [1985] or *Molina and Molina* [1986]), see Figure 5. Therefore as *Kirchhoff et al.* [2002] found, the solar radiation is more dependent on the variation of the ozone absorption coefficient at 306.3 nm than at the other wavelengths. Even if the standard value of the effective ozone temperature is close to the mean effective ozone temperature (see section 4.2), AOD changes a lot if the effective temperature deviates substantially from the mean for particular day. Therefore to eliminate the dependence on the effective ozone temperature, we computed the ozone absorption coefficients using the effective ozone temperature in function of time.

5. Results

5.1. Comparison With AERONET Data Set

5.1.1. A Qualitative Comparison

[52] At Uccle, as the AOD in the UV are not measured with other means, we have to compare our results only qualitatively with results obtained at other stations. The AERONET database gathers AOD measurements inferred from sunphotometers but the AOD is only available for wavelengths greater than 340 nm. AOD measured at Lille (50°36′N, 3°08′E) in France and Ostende (51°13′N, 2°55′E) in Belgium, which are the closest places to Uccle in this
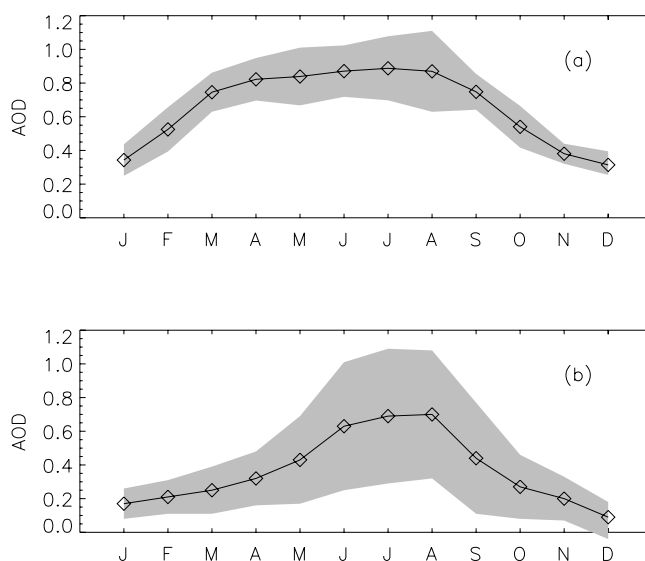
Figure 7. Monthly mean AODs (a) over the period 1984–2002 at Uccle for 320.1 nm and (b) over 1993–2001 at the GSFC for 340 nm.

database, are compared with AOD obtained at Uccle. AERONET results are compared with the nearest Brewer wavelength 320.1 nm. Within this comparison we can only look at the qualitative characteristics of our results: the time variation and the order of magnitude.

[53] Table 6 summarizes the monthly mean AOD for the 3 stations. It shows that all of them are lower than 1.1 over the period June–December. Moreover, *Kirchhoff et al.* [2002] found AOD of about 0.8 at La Paz which is a big city like Brussels near Uccle, in August 1999 at 320.1 nm. At Uccle the calculated AOD is of the same magnitude. Higher values of the AOD than at Lille and Ostende are probably due to the urban pollution.

5.1.2. The Annual Cycle

[54] Figure 6 shows the daily mean AOD from 1984 to 2002 at 320.1 nm. An annual cycle is clearly observed: there is an increase during spring and summer and a decrease in autumn and winter.

[55] Figures 7a and 7b show the monthly mean AOD at Uccle over 1984–2002 and at the GSFC in the United States (39°01′N, 76°52′W) over 1993–2001 for 320.1 nm
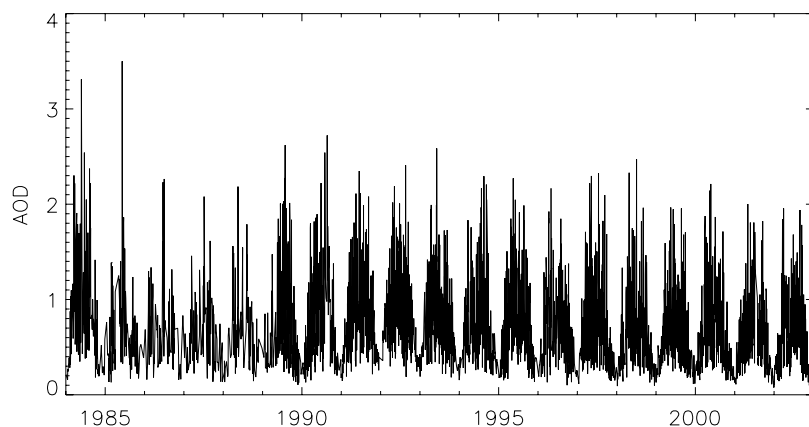
Figure 6. Time series of the daily AOD over the period 1984–2002 at Uccle for 320.1 nm.

and 340 nm (http://aeronet.gsfc.nasa.gov:8080), respectively. The long term monthly mean AOD are calculated from the individual monthly mean AOD for each year. The shaded area is the standard deviation of each month. This seasonal cycle is not a local phenomenon. It is observed in several locations all over the world: *Wenny and Saxena* [2001] observed it in North Carolina, *Wilson and Forgan* [2002] in Tasmania, F. Marenco (oral presentation in the 7th biennial Brewer users group meeting, 2002) at Lampedusa and K. Vanicek (personal communication, 2002) at Hradec Kralove in Czech Republic.

[56] A relation with a pollution cycle or with a general circulation could be an explanation of the annual cycle. The seasonal variation of the mixing layer height could be another explanation: indeed, it is smaller in winter and autumn. Therefore the AOD measured for these seasons could be smaller than in summer and spring where the mixing layer height is thicker.
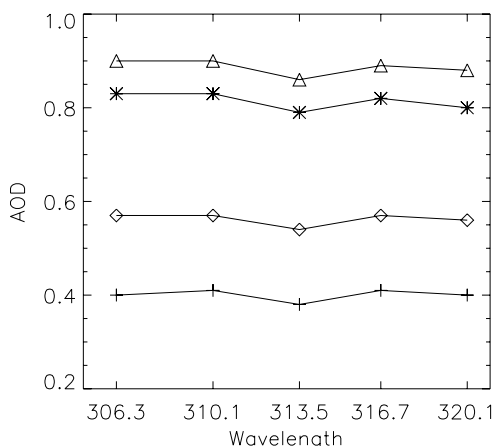
5.2. Variation of the AOD in Function of Wavelength

[57] Figure 8 represents the seasonal monthly mean AOD over the whole period 1984–2002 in function of wavelength. The annual cycle is obvious: the AODs in winter and autumn are lower than in spring and summer. *Angström* [1964] showed that for the wavelengths above 400 nm the AOD decreases when the wavelength increases. In contradiction with *Kirchhoff et al.* [2002] at Campo Grande, the AODs calculated at Uccle have no dependency with wavelength.
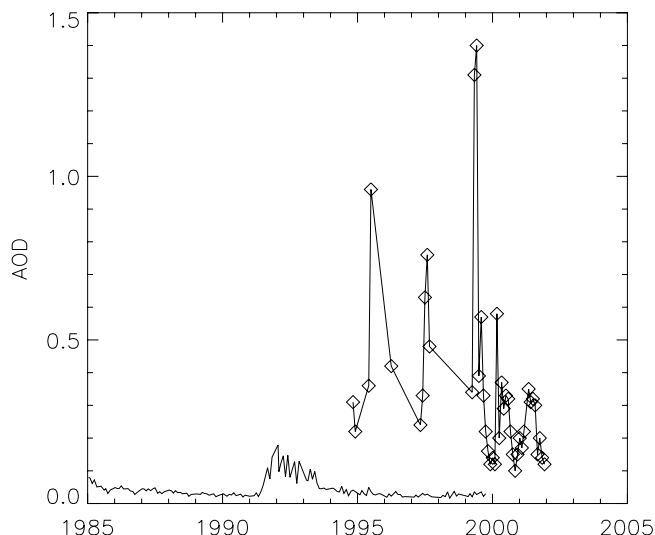
5.3. Pinatubo Eruption Impact

[58] The Pinatubo eruption in June 1991 injected 20 megatons of SO_2 in the stratosphere [*Robock*, 2002]. It caused a decrease of the total ozone at Uccle and many other stations [*De Backer*, 1994; *World Meteorological Organization*, 1992].

[59] Figure 9 shows the monthly mean AOD at Lille from AERONET database at 340 nm (line with diamonds) and in the latitude band between 50°N and 52°N from SAGE II version 6 observations (black line) (http://www-sage2.larc.nasa.gov). In the SAGE II observations, a significant

Figure 9. Comparison between SAGE and AERONET annual monthly mean AOD. Line with diamonds is the AERONET AOD at Lille for 440 nm and the solid line is from SAGE for 452 nm from 10 km to the top of the atmosphere between 50 and 52°N.

increase of the AOD of about 0.15 in the stratosphere is observed at the beginning of 1992 due to the Pinatubo eruption (Figure 9): at 452 nm SAGE II detected an increase of about 300% of the AOD in the stratosphere.

[60] SAGE II measures the extinction coefficient in the stratosphere between 10 and 40 km altitude. On the contrary, the Brewer spectrophotometer at Uccle measures the AOD from the ground to the top of the atmosphere. Figure 6 includes also the period where the Pinatubo aerosols were present in the atmosphere. On this figure, there is no clear signature of the Pinatubo eruption. However, in Figure 10
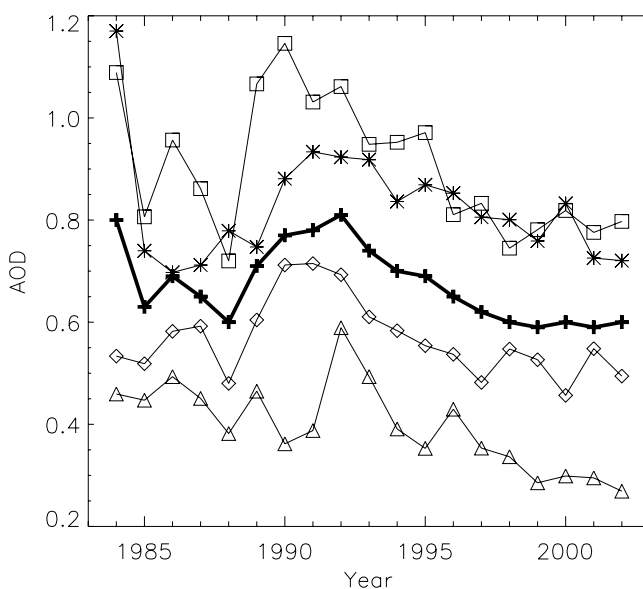
Figure 8. Seasonal means of the AODs at Uccle in function of wavelengths at Uccle over 1984–2002: spring (asterisks), summer (triangles), autumn (diamonds) and winter(crosses).

Figure 10. Annual mean AOD (crosses bold line), summer (square), spring (asterisks), autumn (diamonds) and winter (triangles) from 1984 to 2002 for 306.3 nm.

which shows the seasonal annual mean of AOD, there is an increase of about 0.15 of the AOD in winter 1992 which is in agreement with the AOD's increase observed by SAGE II. The AOD's increase in winter 1992 is seen at all wavelengths. This means that the ozone variation is not related to this AOD's increase (see section 4.1). At Uccle, the impact of the Pinatubo eruption was the largest in February 1992 for ozone [*De Backer*, 1994]. This illustrates the enhanced stratospheric aerosol load after the Pinatubo's eruption in winter. To conclude, we infer that this AOD's increase is due to the Pinatubo eruption. The lack of any signal in other seasons and on the annual mean AOD is probably due to the fact that with the observations from the ground we measure mainly tropospheric aerosols in the urban pollution layer, having a high variability during most of the year.

[61] Owing to the large AOD's variation, an increase of about 0.15 as observed by the SAGE II instrument caused by the Pinatubo eruption impact, cannot be observed with our Brewer spectrophotometer from the ground for most of the year.

5.4. Trends of the AOD

[62] Trends are an essential element in the climate change. They give us information to understand how our climate changes. As the impact of the Pinatubo eruption is negligible for the largest part of the year at Uccle, the trends can be computed for the whole period 1984–2002. First, we study the annual trend and afterwards the seasonal trend. We use a least chi-square linear regression to compute the trend and we express it in %/year. The trends are computed from the monthly mean AOD over the period 1984–2002. The slope of the linear regression is divided by the mean AOD over the whole period and finally multiplied by 100 to obtain trends in %/year.

5.4.1. Annual Trend

[63] Figure 11 shows the time variation of the annual mean AOD (line with diamonds) for the period 1984–2002 for the 2 wavelengths: 306.3 nm and 320.1 nm. The black
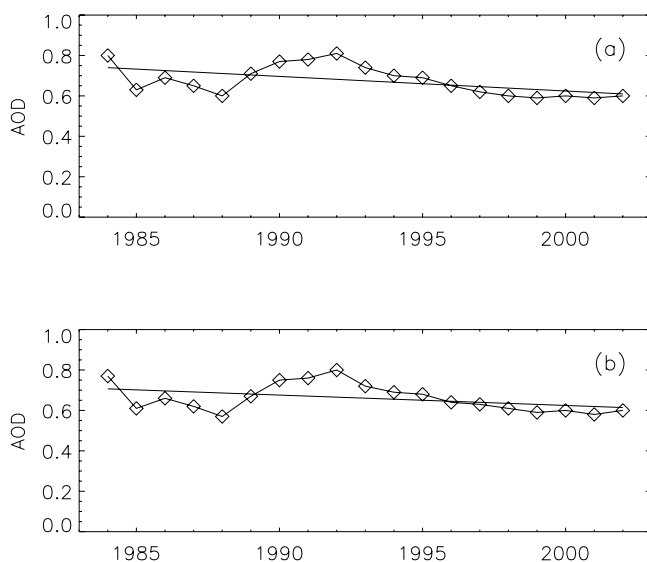
Table 7. Annual Trend of the AODs for the 5 Brewer Wavelengths at Uccle From the Annual Mean AOD Calculated From the Monthly Mean AOD for the Period 1984–2002 and 1989–2002

Wavelength, nm	Trend, %/year 1984–2002	Trend, %/year 1989–2002
306.3	−1.07 ± 0.41	−2.46 ± 0.37
310.1	−0.70 ± 0.39	−1.93 ± 0.35
313.5	−0.44 ± 0.40	−1.71 ± 0.33
316.7	−0.51 ± 0.40	−1.75 ± 0.35
320.1	−0.78 ± 0.42	−2.13 ± 0.39

line represents the least chi-square linear regression. Table 7 summarizes the trends of the 5 wavelengths for two periods: 1984–2002 and 1989–2002. The annual mean trend over the period 1989–2002 clearly shows a negative significant trend which is more pronounced than over 1984–2002 at all wavelengths, see Table 7, while for 1984–2002, there is only a significant trend at 306.3 nm.

5.4.2. Seasonal Trend

[64] Trends are also calculated for four seasons defined as: spring (March, April, May), summer (June, July, August), autumn (September, October, November), and winter (December, January, February).

[65] Table 8 summarizes all the trends for these seasons. The absolute values of the trends are lowest (and almost zero) during spring and autumn. More important, always negative, trends are only significant at the 2σ level for winter at all wavelengths and at 306.3 nm in summer. The winter trend is probably due to the Pinatubo eruption impact which increased the AOD in 1992.

5.4.3. Summary of the Annual and Seasonal Trends

[66] Figure 10 represents the annual and seasonal mean AOD as a function of time from 1984 to 2002 from the monthly mean AOD. A decrease in the annual mean AOD is observed from 1984 to 1988. This decrease is caused by variations during spring and summer, while autumn and winter AODs were almost constant during the period.

6. Conclusions

[67] The Langley Plot Method is tested on the long time series of Brewer #16 DS observations at Uccle from 1984 to 2002. This time series gives us the opportunity to compute a long time series of AOD in the UV-B at Uccle using direct solar irradiance measurements.

[68] We introduce in this work the effective ozone temperature dependence of the ozone absorption coefficient. We observed that the AOD is sensitive to the use of an effective temperature while it is less the case for the CF. Thus the effective ozone temperature dependence is taken

Figure 11. Annual trend of the AODs at (a) Uccle for 306.3 nm and (b) 320.1 nm at Uccle from 1984 to 2002.

Table 8. Seasonal Trend From the Mean Annual AOD for the Five Brewer Wavelengths in %/year From 1984 to 2002

Wavelength, nm	Spring March/ April/May	Summer June/ July/Aug.	Autumn Sep./ Oct./Nov.	Winter Dec./ Jan./Feb.
306.3	−0.61 ± 0.56	−1.24 ± 0.55	−0.77 ± 0.54	−2.66 ± 0.65
310.1	−0.25 ± 0.56	−0.88 ± 0.53	−0.39 ± 0.51	−2.18 ± 0.61
313.5	0.04 ± 0.59	−0.62 ± 0.54	−0.09 ± 0.52	−2.01 ± 0.66
316.7	−0.06 ± 0.57	−0.69 ± 0.53	−0.17 ± 0.51	−1.98 ± 0.61
320.1	−0.33 ± 0.59	−0.99 ± 0.55	−0.47 ± 0.55	−2.30 ± 0.65

into account in order to avoid the small errors that arise from using a constant effective ozone temperature.

[69] The ozone's error contribution to AOD error is important at 306.3 nm but not at the other wavelengths compared to the error on CF to AOD error which is 0.03.

[70] The magnitude of the retrieved AODs compares well with other studies. Also an annual cycle is found in the data set at Uccle. This is not a local phenomenon because it was observed in other places all over the world.

[71] Besides the comparisons of the AOD obtained by this method with those from other sources, the time evolution of AOD was analyzed. The impact of the Mount Pinatubo eruption in 1991 is only discernible at Uccle in the UV-B in winter. Because of the large AODs variability during most of the year, this impact is not visible in the other seasons and on the mean annual AOD. This suggests that the retrieved AODs are dominated by tropospheric aerosols.

[72] Our results suggest that in the UV-B the AOD do not depend on wavelength at Uccle. It is in contradiction with *Kirchhoff et al.*'s [2002] result: he found a dependency between the AOD and the wavelength but it is in contradiction with Angström's results for wavelengths above 400 nm.

[73] We derived trends of AOD for the different wavelengths and for different seasons. Over the period 1984 to November 2002, there is no significant annual trend except at 306.3 nm. However, over the period 1989–2002, a significant negative trend at the 2σ level is clearly observed at all five wavelengths and it is more negative than from 1984 to 2002. In winter at all wavelengths and in summer at 306.3 nm, the trends are significant at the 2σ level. For the other seasons, no significant trend is observed. We notice that in summer even the trend is not significant at 4 wavelengths, the trends are more consistent than in spring and autumn. The explanation of these trends will be the subject of a future study.

References

Alexandrov, M. D., A. A. Lacis, B. E. Carlson, and B. Cairn, Remote sensing of atmospheric aerosols and trace gases by means of multifilter rotating shadowband radiometer: Part I. retrieval algorithm, *J. Atmos. Sci.*, 59, 524–543, 2001.

Angström, A., The parameters of atmospheric turbidity, *Tellus*, 16, 64–75, 1964.

Bais, A. F., Absolute spectral measurements of direct solar ultraviolet irradiance with a Brewer spectrophotometer, *Appl. Opt.*, 36, 5199–5204, 1997.

Bass, A. M., and R. J. Paur, The ultraviolet cross-sections of ozone, I, The measurements, in *Atmospheric Ozone*, edited by C. S. Zerefos and A. Ghazi, pp. 606–610, D. Reidel, Norwell, Mass., 1985.

Brewer, A. W., A replacement for the Dobson spectrophotometer, *Pure Appl. Geophys.*, 106–108, 919–927, 1973.

Cachorro, V. E., R. Vergaz, M. J. Martin, A. M. de Frutos, J. M. Vilaplana, and B. de la Morena, Measurements and estimation of the columnar optical depth of tropospheric aerosols in the UV spectral region, *Ann. Geophys.*, 20, 565–574, 2002.

De Backer, H., Analysis and interpretation of ozone observations at Uccle (1969–1993), Ph.D. Thesis, Vrije Univ., Brussels, 1994.

De Backer, H., and D. De Muer, Intercomparison of total ozone data measured with Dobson and Brewer ozone spectrophotometers at Uccle (Belgium) from January 1984 to March 1991, including zenith sky observations, *J. Geophys. Res.*, 96, 20,711–20,719, 1991.

De Muer, D., and H. De Backer, Revision of 20 years of Dobson total ozone data at Uccle (Belgium): Fictitious dobson total ozone trends induced by sulfur dioxide trends, *J. Geophys. Res.*, 97, 5921–5937, 1992.

Houghton, J. T., Y. Ding, D. J. Griggs, M. Noguer, P. J. van der Linden, D. Xiaosu, K. Maskell, and C. A. Johnson (Eds.), *Climate Change 2001: The Scientific Basis*, 896 pp., Cambridge Univ. Press, New York, 2001.

King, M. D., D. M. Byrne, J. A. Reagan, and B. M. Herman, Spectral variation of optical depth at Tucson, Arizona between August 1975 and December 1977, *J. Appl. Meteorol.*, 19, 723–732, 1980.

Kirchhoff, V. W. J. H., A. A. Silva, C. A. Costa, N. Paes Lem, H. G. Pavao, and F. Zaratti, UV-B optical thickness observations of the atmosphere, *J. Geophys. Res.*, 106, 2963–2973, 2001.

Kirchhoff, V. W. J. H., A. A. Silva, and D. K. Pinheiro, Wavelength dependence of aerosol optical thickness in the UV-B band, *Geophys. Res. Lett.*, 29(12), 1620, doi:10.1029/2001GL014141, 2002.

Krishna Moorthy, K., S. K. Satheesh, and B. V. Krishna Murthy, Characteristics of spectral optical depths and size distributions of aerosols aver tropical oceanic regions, *J. Atmos. Sol. Terr. Phys.*, 60, 981–992, 1998.

Kylling, A., A. F. Bais, M. Blumthaler, J. Schreder, C. S. Zerefos, and E. Kosmidis, Effect of aerosols on solar UV irradiances during the photochemical activity and solar ultraviolet radiation campaign, *J. Geophys. Res.*, 103, 26,051–26,060, 1998.

Liu, S. C., S. A. McKeen, and S. Madronich, Effect of anthropogenic aerosols on biologically active ultraviolet radiation, *Geophys. Res. Lett.*, 18, 2265–2268, 1991.

Marenco, F., V. Santacesaria, A. F. Bais, D. Balis, A. di sarra, A. Papayannis, and C. Zerefos, Optical properties of tropospheric aerosols determined by lidar and spectrophotometric measurements (photochemical activity and solar ultraviolet radiation campaign), *Appl. Opt.*, 36, 6875–6886, 1997.

Marenco, F., A. di Sarra, and J. De Luisi, Methodology for determining AOD from Brewer 300–320-nm ozone measurements, *Appl. Opt.*, 41, 1805–1814, 2002.

Molina, L. T., and M. J. Molina, Absolute absorption cross-sections of ozone in the 185- to 350 nm wavelength range, *J. Geophys. Res.*, 91, 14,501–14,508, 1986.

Petters, J. L., V. K. Saxena, J. R. Slusser, B. N. Wenny, and S. Madronich, Aerosol single scattering albedo retrieved from measurements of surface UV irradiance and a radiative transfer model, *J. Geophys. Res.*, 108(D9), 4288, doi:10.1029/2002JD002360, 2003.

Robock, A., The climate aftermath, *Science*, 295, 1242–1244, 2002.

SCI-TEC, Brewer ozone spectrophotometer, Acceptance manual, Document number AM-BA-C05-Rev C, SCI-TEC Instruments, 1988.

Takemura, T., T. Nakajima, T. Nozawa, and K. Aoki, Simulation of future aerosol distribution, radiative forcing, and long-range transport in east Asia, *J. Meteorol. Soc. Jpn.*, 79, 1139–1155, 2001.

Van Roozendael, M., et al., Validation of ground-based visible measurements of total ozone by comparison with Dobson and Brewer spectrophotometers, *J. Atmos. Chem.*, 29, 55–83, 1998.

Wenny, B. N., and V. K. Saxena, Aerosol optical depth measurements and their impact on surface levels of ultraviolet-B radiation, *J. Geophys. Res.*, 106, 17,311–17,319, 2001.

Wilson, S. R., and B. W. Forgan, Aerosol optical depth at Cape Grim, Tasmania, 1986–1999, *J. Geophys. Res.*, 107(D8), 4068, doi:10.1029/2001JD000398, 2002.

World Meteorological Organization, Scientific assessment of stratospheric ozone: 1989, *Rep. 25*, pp. 2.1–2.33 and 7.1–7.28, Global Ozone Res. and Monit. Proj., Geneva, 1992.

————————————

A. Cheymol and H. De Backer, Royal Meteorological Institute of Belgium, Av. Circulaire, 3, B-1180 Brussels, Belgium. (anne.cheymol@oma.be; hugo.debacker@oma.be)